Effect of Fluorenone Units on the Property of Polyfluorene and Oligofluorene Derivatives: Synthesis, Structure−Properties Relationship, and Electroluminescence

Xing-Hua Zhou, Yong Zhang, Yu-Qing Xie, Yong Cao,* and Jian Pei*

The Key Laboratory of Bioorganic Chemistry and Molecular Engineering of Ministry of Education, College of Chemistry and Molecular Engineering, Peking University, Beijing 100871, China, and Institute of Polymer Optoelectronic Materials and Devices, South China University of Technology, Guangzhou 510640, China

Received January 18, 2006; Revised Manuscript Received March 28, 2006

ABSTRACT: A series of well-defined 9,9′-dihexylfluorene-*co*-fluorenone copolymers with various fluorenone contents and a set of monodisperse oligofluorenes in the chain center have been developed through the palladium-catalyzed Suzuki coupling reaction. The structure−property relationships, especially the effect of fluorenone moieties on the photophysical and electroluminescent properties of these materials, are systematically investigated to elucidate the exact origin of the low-energy emission in polyfluorenes. On the basis of our substantial studies of the steady-state photoluminescence (PL) and PL decay dynamics of the fluorenone-containing oligomers and copolymers both in dilute solutions and in thin films, the origin of the controversial low-energy emission band might be due to the interaction between intrachain fluorenone moieties in polyfluorenes instead of the intermolecular aggregates or excimers. We further show that fluorene pentamer with a central fluorenone unit (oligomer **2**) is more appropriate to represent the actual chromophore responsible for the green emission in the copolymers. The green emission of the copolymers in the solid states is well described by single-exponential decay and has a lifetime ranging from 4.21 to 8.15 ns, depending on fluorenone content. The substantially enhanced intensity of the green emission with increasing the intermolecular interaction in solid states results from the contribution of both the intramolecular and the more efficient intermolecular energy transfer from the fluorene segments to fluorenone moieties. We also find that the emission wavelength and the lifetime of the green emission for the copolymer with the lowest fluorenone content (**PHF-FO0.1**) in solid states are very similar to those of the emerging low-energy emission for poly(9,9′-dihexylfluorene) (**PDHF**) after high-temperature thermal annealing in air. Bright yellow electroluminescence (EL) is achieved from double-layer LEDs based on these materials with an emission peak of 540−579 nm that steadily red-shifted with increasing fluorenone contents. The better luminance and external quantum efficiencies are probably due to improved electron injection and carrier transporting as well as efficient charge trapping and recombination at the fluorenone sites.

Introduction

Oligofluorenes and polyfluorenes (PFs) are generally regarded as the most promising candidates for blue light-emitting active layers in organic light-emitting devices (OLEDs) due to their high thermal stability and exceptionally high solid-state photoluminescence quantum yields as well as good charge transport properties.[1] However, OLEDs fabricated from PF derivatives suffer from a degradation of the device under operation that is documented in the formation of a low-energy emission band at 500−600 nm turning the desired blue emission color into the undesired blue-green emission.[2] This band is also found in photoluminescence as a result of photodegradation and/or thermal annealing in air. Despite the ongoing improvements in terms of stability and color purity of PF-based LEDs, the true nature of the origin of this long wavelength emission has been controversial and is not still fully understood.

Before 2002, the low-energy emission band was mostly attributed to reorganization of polymer chains and subsequent aggregate[3] and/or excimer formation.[2a,c] This assumption has seemingly been confirmed by the success of attempts to stabilize the blue emission of PFs through various modifications to the inhibition of interchain interactions.[4−7] However, List et al.[2d] proposed that the low-energy emission was rather related to electro- and photooxidative degradation processes, giving rise to ketone defects incorporated into the polymer backbone. The ketone functionalities were identified by ultraviolet−visible (UV−vis), photoluminescence (PL) emission, and infrared (IR) spectroscopy. Such a hypothesis is strongly supported by the distinct changes of PL spectra of PF films after high-temperature annealing under different conditions. For example, the significant contribution of green emission showed in air; however, no obvious change was observed in an inert atmosphere or in vacuo.[2e,8,9] The observation of the low-energy emission band in decayed PL measurements on dilute solutions of a range of poly- and oligofluorenes also favored such notion.[10] Moreover, recent results from time-gated electroluminescence (EL) spectroscopy of PF LEDs also demonstrated the effect of on-chain ketone defects rather than excimers as charge carrier traps on emission properties of PFs.[11]

To gain a deeper insight into the impact of ketone defects on the optical and electronic properties and further allow clarification of the exact nature of the low-energy emission, a considerable body of work has been devoted to the study of dialkylfluorene-based copolymers containing a well-defined fraction of the fluorenone unit as model systems for degraded PF.[8b,12] Few research results demonstrated that the low-energy emission band could be directly excited with monoexponential decay kinetics and similar to the reported troublesome green band in PFs observed in very dilute solutions of the fluorenone-containing

* Corresponding authors. E-mail: jianpei@pku.edu. cn; poycao@scut.edu.cn.

10.1021/ma0601262 CCC: $33.50
Published on Web 05/03/2006

Chart 1

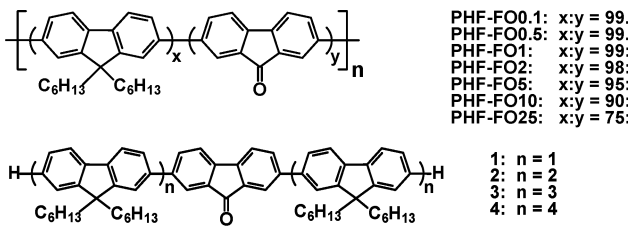

copolymers.[8b,12] Such results were directly *against* the idea that excimer or aggregate formation is the primary source for the low-energy emission band in PF derivatives. On the contrary, they strongly supported the assignment of emissive on-chain ketone defects for such a green band. However, Bradley et al.[13] thought that interchain/intersegment interactions played an essential role in green band emission and proposed that the green band arose from fluorenone-based excimers rather than the on-chain ketone defects. To date, although the key role of ketone defects in the photophysics of PFs has been confirmed, the debate about the exact nature of the low-energy emission band in PFs is still going on. Further investigations are needed to elucidate the exact origin of this emission since it is vital to overcome this problem and to provide suitable future synthetic strategies.

In this contribution, we present the synthesis and study of the photophysical proerties as well as EL properties of a series of well-defined fluorenone-containing oligo- and polyfluorene derivatives. Their structures are shown in Chart 1. We also synthesize four monodisperse oligofluorene derivatives with one central fluorenone unit, which serve as the model systems for our dihexylfluorene−fluorenone copolymers to understand the exact chromophore involved in the low-energy emission band. The structures of all these compounds are fully characterized. We also systematically investigate the photophysical properties and time-resolved PL decay dynamics of these materials both in dilute solutions and in solid states. Double-layer LEDs using these materials as emissive layers exhibit bright yellow EL, which make them promising candidates for OLED.

Results and Discussion

Synthesis. The well-defined fluorenone-containing oligo- and polyfluorene derivatives were synthesized by the Suzuki cross-coupling raction.[14] The synthetic route is illustrated in Scheme 1. The growth of the oligofluorene chain commenced with 2,7-dibromofluorenone and thereafter monomer **M1** was added in a repetitive stepwise fashion to couple with the corresponding dibromide derivatives, which successfully afforded oligomers **1**−**4** in high yields. It should be pointed out that Yamamoto coupling reaction under harsh conditions for the preparation of such copolymers inevitably incorporated oligomeric fluorenone segments into the polymer chains, especially in high feed ratios of fluorenone.[8b,12a−e] In contrast, the Suzuki coupling polymerization was characteristic of generating well-defined alternating molecular structures with each 9-fluorenone moiety being isolated within the polymer chains.[12f] In our experiments, copolymers with the fluorenone content in the range of 0.1−25 mol %, **PHF-FO0.1**−**25**, were synthesized by Suzuki coupling polymerization in good yields (Scheme 1). It is noteworthy that we chose compound **1a** instead of 2,7-dibromoflurenone due to its improved solubility and similar reactivity to 2,7-dibromo-9,9-dihexylfluorene, thus ensuring the real content of fluorenone in the desired copolymers close to the value of the monomer feed ratio. Poly(9,9′-dihexylfluorene) (**PDHF**) was also prepared for comparison.

All of these oligomers and copolymers were readily soluble in common organic solvents such as chloroform, THF, and toluene, and their molecular structures were verified by ^{1}H and ^{13}C NMR spectroscopy, elemental analysis, and FT-IR spectroscopy. The incorporation of the fluorene unit into the copolymer backbone was indicated by the observation of their characteristic signals and their clear assignments in the NMR and FT-IR spectra. For example, a peak at around 8.06 ppm in ^{1}H NMR spectra was assigned to the aromatic proton in the fluorenone ring. In their ^{13}C NMR spectra, seven peaks at ca. 194.2, 142.9, 142.6, 138.5, 135.2, 133.3, and 123.1 ppm was assigned to the carbons of the fluorenone ring. In FT-IR spectra, the vibration band at 1720 cm^{-1} was associated with C═O stretch from the fluorenone moiety. However, these characteristic peaks were not observed for the samples with the concentration of fluorenone moiety less than 2 mol %. The molecular weights for oligomers **1**−**4** were also characterized by MALDI-TOF MS measurement. The number-average molecular weights (M_n) of the copolymers, obtained by gel permeation chromatography (GPC) using THF as the eluent and polystyrene as standards, ranged between 7300 and 12 200 with a polydispersity index of 1.48−2.96.

Thermal Analysis. The thermal properties of the oligmers and copolymers were evaluated by thermogravimetric analysis (TGA) and differential scanning calorimetry (DSC) under a nitrogen atmosphere. The results are presented in Table 1. All materials exhibited an onset of decomposition greater than 400 °C with no weight loss at lower temperature, suggesting their outstanding thermal stability. TGA experiments showed major weight loss in the range of 410−500 °C and further mass stability until 700 °C. After thermal annealing upon the first heating to 300 °C, only glass transitions were observed, and no crystallization and melting peak were observed upon heating above the glass transition temperature. The glass transition temperatures (T_g) of oligomers **1**−**4** were improved from 45 to 80 °C with an increase of the conjugation length. Homopolymer **PDHF** and copolymers **PHF-FO0.1-5** showed glass transitions at around 104 °C, while **PHF-FO10** and **PHF-FO25** had higher glass transition at 120 and 142 °C, respectively. The results showed that an increase of the content of rigid fluorenone moiety effectively improved the T_g of polymers.

Steady-State Optical Properties. The normalized absorption and PL emission spectra of oligomers **1**−**4** in dilute THF solutions (10^{-6} M) are shown in Figure 1. The optical absorption spectra showed that the absorption maximum (λ_{max}) of oligomers **1**−**4** was located at 350, 367, 373, and 378 nm, respectively, exhibiting a progressive red shift with an increase of the fluorene components. This was quite similar to other monodisperse fluorenone-containing derivatives both in solutions and in the films.[11] The absorption λ_{max} of **1**−**4** was quite close to that of the corresponding oligo(9,9′-dihexylfluorene)s with the same chain length,[15] which indicates that this band was associated with the $\pi-\pi^*$ transition of the entire molecular backbone for **1**−**4**, and there was no interruption in the π-conjugation between fluorene and fluorenone rings. A weak absorption band at about 450 nm (ca. 2.76 eV) was observed in the low-energy wing of the main absorption band, the absorption strength of which decreased as the fluorenone content decreased from **1** to **4** (see the inset of Figure 1). This low oscillator strength band has been assigned to a charge transfer (CT) n$-\pi^*$ transition of fluorenone segments.[12c] The absorption λ_{max} of this band was shifted toward longer wavelengths in comparison with that of fluorenone (λ_{max} = 375 nm).[12b] However, such absorption λ_{max}

Scheme 1[a]

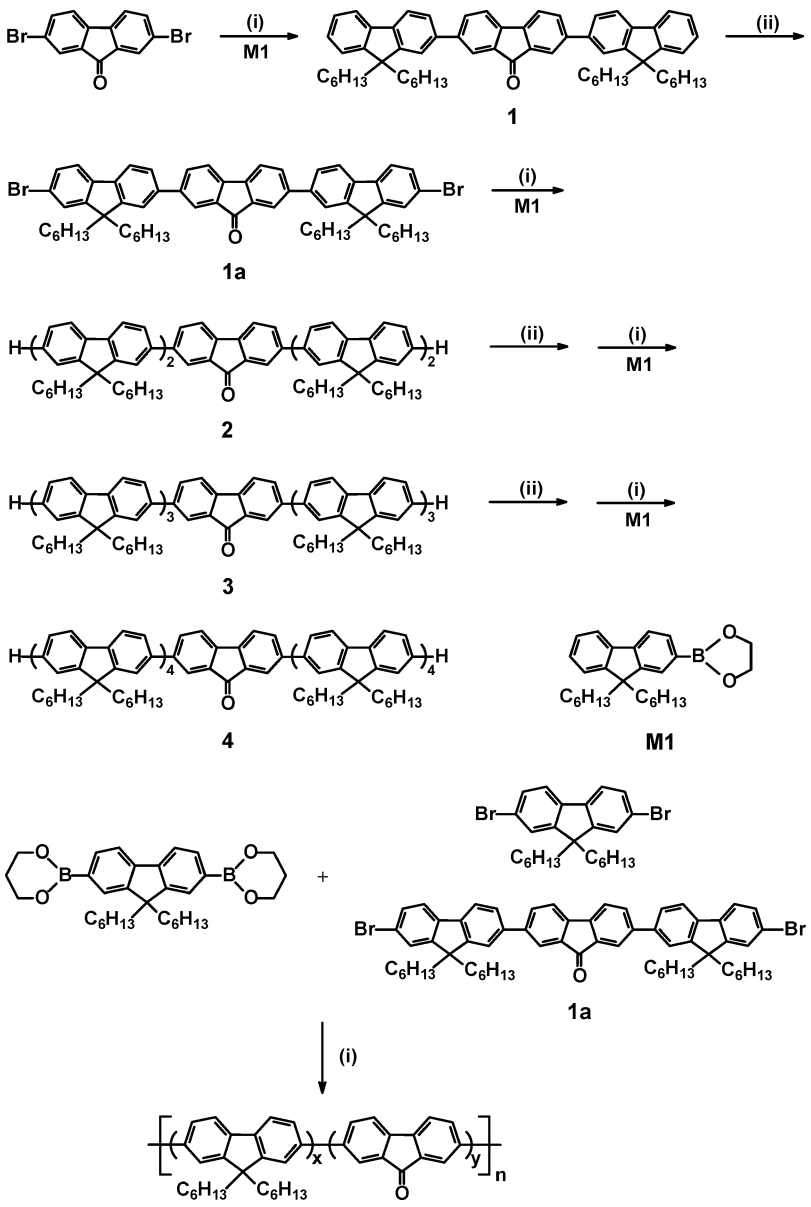

[a] (i) $Pd(PPh_3)_4$, 2 M Na_2CO_3, toluene, 90 °C; (ii) $CuBr_2-Al_2O_3$, CCl_4, reflux.

Table 1. Molecular Weights and Thermal Properties of the Fluorene-Containing Oligo- and Polyfluorene Derivatives

compd	M_n	M_w/M_n	T_g (°C)	T_d (°C)
1	844.8		45	411
2	1508.8		60	426
3	2173.0		78	426
4	2831.6		80	426
PDHF	12100	2.85	104	427
PHF-FO0.1	12200	2.96	104	421
PHF-FO0.5	7300	1.48	104	427
PHF-FO1	9200	1.79	104	427
PHF-FO2	8500	1.84	104	426
PHF-FO5	9500	1.99	104	429
PHF-FO10	11100	2.39	120	427
PHF-FO25	11700	2.65	142	428

did not exhibit obvious change with the elongation of the oligofluorene backbone.

The PL emission spectra of **1**−**4** in dilute THF solutions, excited at absorption maximum, showed two spectral contributions: a dominant unstructured green emission band centered at around 520 nm and a structured blue band resulting from the regular oligofluorene luminescence. We observed that the characteristic blue emission was suppressed significantly and substantially weaker than the low-energy emission, especially for **1**, **2**, and **3**. For **4**, the blue band at 402 nm recovered to some extent but was still merely 55% as intense as the green band at 523 nm. The dominant green band at about 520 nm, with a red shift of ca. 8 nm occurring from **1** to **4**, was recognized as the feature often found in the PL spectra of annealed or degraded PF films, even more pronounced in the electroluminescence spectra of PF.[2] The occurrence of this emission in dilute solutions suggested that this emission band did not originate from intermolecular aggregates or excimers, which was also supported by the facts that direct excitation at 450 nm resulted in an identical low-energy emission with the intensity decreasing significantly due to the weak absorption strength at this wavelength. Thus, this green emission band was unambiguously related to the fluorenone moiety in isolated chains. Using calculations, Zojer et al.[12c] have demonstrated that it originated from a emissive charge transfer (CT) $n-\pi^*$ state strongly confined to the fluorenone unit. An occurrence of intramolecular energy transfer from fluorene segments, acting as excitation donors, to fluorenone moieties as excitation

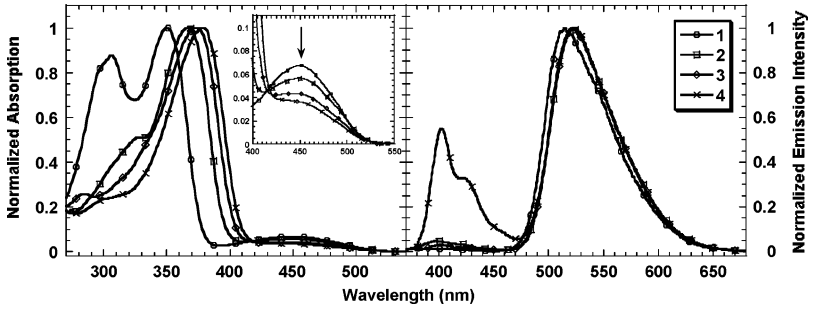

Figure 1. Normalized absorption and PL emission spectra of oligomers **1**−**4** in THF solutions (10^{-6} M) at room temperature.

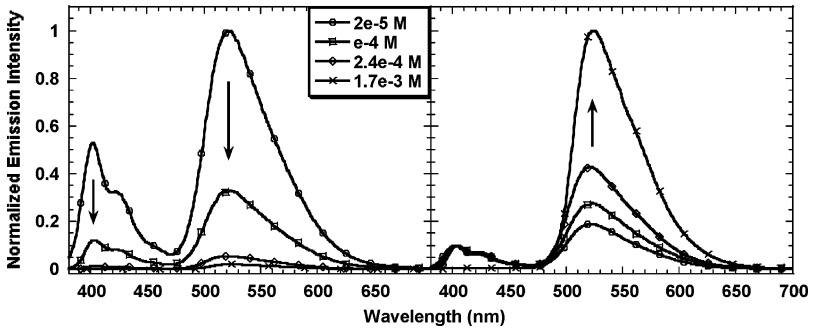

Figure 2. Evolution of the PL emission spectra of oligomer **4** in THF solutions as the solution concentration is increasing.

acceptor must be responsible for the PL spectral characteristics of these oligomers. But such intramolecular energy transfer was insufficient to quench the blue emission for those molecules with the chain length equal to or longer than that of oligomer **4** in dilute solutions.

To further investigate the concentration dependence of the PL emission of the oligomers, we measured the PL spectra of **4** in THF solutions at different concentrations ranging from 2×10^{-5} to 1.7×10^{-3} M, as shown in Figure 2. We observed that both the blue emission and the green emission were sufficiently quenched as the concentration increased. On the other hand, from the PL spectra normalized to the blue peak (see the right panel in Figure 2), we also noted that the *relative* intensity of the green emission band was enhanced with increasing solution concentration, and the blue emission band nearly vanished at a concentration of 1.7×10^{-3} M. The remarkable enhancement of the relative intensity of the green emission band might be because of more efficient intermolecular energy transfer favored by increasing solution concentration.

Moreover, the PL emission spectra of the oligomers also showed a distinct solvent dependence. This effect was documented in Figure 3, where the PL spectra were presented for dilute solutions of **4** in solvents of varying polarity. In agreement with the results of the fluorenone copolymers by Romarner et al.,[8b] we observed that the spectral position and strength of the blue emission band were hardly affected by the solvent, with the largest shift of 5 nm toward shorter wavelengths in hexane. In contrast, the green emission band showed a strong bathochromic shift (ca. 47 nm) with increasing solvent polarity, indicating a strong polar emissive state based on the flourenone moiety. Meanwhile, the relative intensity of the green emission band was substantially reduced. The most drastic effect is observed in solvents such as chloroform, dichloromethane, and methanol, where the green emission band is barely detectable.

The normalized absorption and PL spectra of the dihexylfluorene−fluorenone copolymers **PHF-FO0.1**−**25** in dilute THF solutions (10^{-5} M) are depicted in Figure 4. We observed that the dominant absorption band peak at around 380 nm, which corresponded to the singlet $\pi-\pi^*$ transition of the polyfluorene

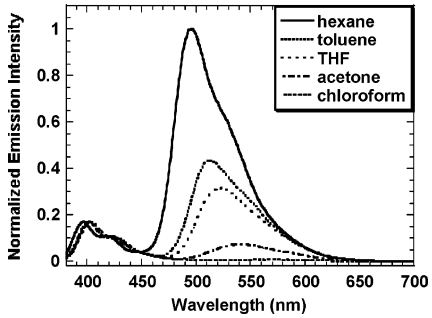

Figure 3. Normalized PL emission spectra of oligomer **4** in different solvents (10^{-5} M).

backbone, showed a small blue shift of about 6 nm in comparison with poly(9,9′-dihexylfluorene). The weak broad peak at about 450 nm similar to that of the oligomers was slightly enhanced with an increase in fluorenone content from **PHF-FO0.1** to **PHF-FO25**. Their PL spectra showed that the low-energy emission grew progressively in intensity with a peak fixed at about 520 nm at the expense of the efficient blue emission ($\lambda_{max} = 402$ nm) when the fluorenone content in the copolymers increased. The copolymers containing lower than 2 mol % fluorenone moieties exhibited almost the same PL spectra and similar emission intensity (from the PL spectra normalized to the absorption) as those of **PDHF**; however, **PHF-FO2**, **PHF-FO5**, and **PHF-FO10** exhibited an additional broad peak at about 520 nm with a concomitant decrease of the intensity of the blue emission peak, and this long wavelength peak became the maximum in **PHF-FO25**. The complete absence of fluorenone-related emission peaks for the copolymers with lower fluorenone content demonstrated inefficient intrachain energy transfer despite the π-conjugated character of the polyarylene main chain. Similar to the oligomers, the low-energy emission of these copolymer solutions also exhibited a strong dependence on solution concentration and solvent polarity.

The normalized absorption and PL emission spectra of oligomers **1**−**4** and the emission spectra of copolymers **PHF-FO0.1**−**25** as well as **PDHF** in films spin-coated from toluene solutions (2% w/v) are displayed in Figures 5 and 6, respec-

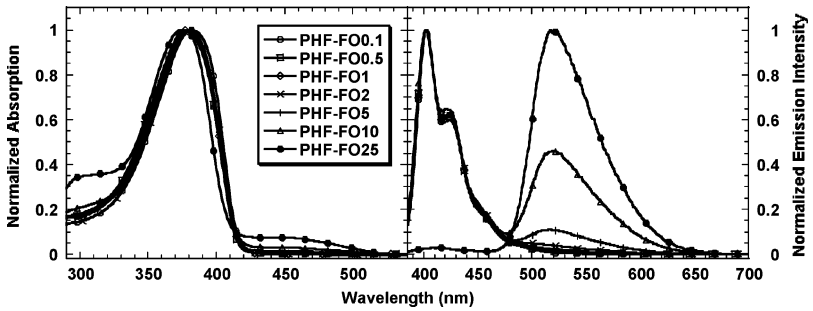

Figure 4. Normalized absorption and PL emission spectra of copolymers **PHF-FO0.1−25** in THF solutions (10^{-5} M) at room temperature.

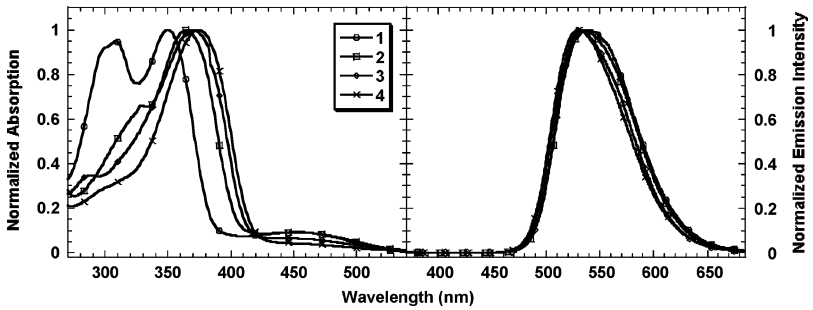

Figure 5. Normalized absorption and PL emission spectra of oligomers **1−4** in the solid state at room temperature.

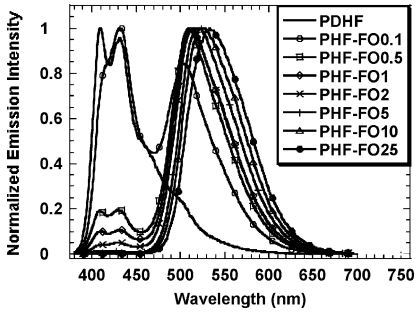

Figure 6. Normalized PL emission spectra of **PDHF** and copolymers **PHF-FO0.1−25** in the solid state at room temperature.

tively. The absorption spectra of both oligomers and polymers in solid states were quite similar to those in dilute solutions, except for the little blue shift; however, their PL emission spectra in films exhibited dramatic changes compared with those in solutions. For the PL spectra of oligomers **1−4**, the green emission band peak at around 535 nm dominated and the blue emission band vanished. The PL spectra of thin films of the polymers gave us a clear picture about the evolution of PL emission spectra with variation of fluorenone content in these polymers (Figure 6). **PDHF** exhibited the typical spectral features of polyfluorene homopolymer and showed blue emission with two vibronic peaks at 409 and 431 nm, which were slightly red-shifted compared with those in the solution. An additional emission band at 504 nm was observed for **PHF-FO0.1** with the fluorenone content as low as 0.1 mol %, the intensity of which was comparable to that of the blue component. When further fluorenone content was increased in copolymers, the green emission dominated and the blue emission was substantially quenched and steadily decreased and was already barely discernible for **PHF-FO5**. In the meantime, the green emission peaks were significantly red-shifted from 504 nm for **PHF-FO0.1** to 533 nm for **PHF-FO25** due to the fact that the aggregation at the excited states was easily formed with the increase of the fluorenone content. It should be pointed out that we found that the green emission peak for **PHF-FO0.1** was identical to the new emerging one of **PDHF** after high-temperature thermal annealing in air. By comparing PL spectra both in solutions and in the solid states, we noted that the relative intensity of the green emission to the blue component in the solid states was remarkably enhanced compared to that in solutions, especially at low fluorenone content, which clearly indicated the importance of interchain interaction and the key role of interchain excitation energy transfer occurring in this case.

Both oligomers and copolymers emitted yellow light in thin films. The absolute PL efficiency of all compounds was measured in the integrating sphere under excitation of 325 nm line of the He−Cd laser. For oligomers, the PL efficiency was improved from 19% for **2** to 46% for **4** with decreasing fluorenone content. The PL efficiency of copolymers initially enhanced with increasing fluorenone content, reaching a maximum of 56% for **PHF-FO1**. With further increasing of the fluorenone content to more than 5 mol %, the PL efficiency started decreasing. Similar behavior of the PL efficiency in thin films was also observed in polyfluorene derivatives incorporated with various narrow-band-gap comonomers.[16] Table 2 summarizes the optical absorption and PL emission spectral properties as well as the absolute PL efficiency of all compounds.

Time-Resolved Photoluminescence Decay Dynamics. The fluorescence decay parameters of our materials both in solutions and in thin films are collected in Table 3. All materials were excited with the maximum absorption wavelengths. In dilute THF solutions (10^{-5} M), the decay of the blue emission band for oligomer **4** and the copolymers was found to be single-exponential with a lifetime ranging from 0.43 to 0.55 ns, which was in agreement with that in the literature.[17] Given the lack of interchain interactions in dilute solutions, this emission was assigned to intrachain singlet excitons on the oligo- and polyfluorene backbone. With increasing fluorenone content from **PHF-FO0.1** to **PHF-FO10**, the lifetime of the blue emission slightly increased. On the other hand, the green emission at about 520 nm for all oligomers and copolymers **PHF-FO2** to **PHF-FO25** had a much longer lifetime (~7 ns) by a single exponential. In comparison with that of **1** (τ = 8.13 ns), the green emission band for oligomers **2**, **3,** and **4** possessed a slightly shorter lifetime of 6.95, 6.63, and 6.67 ns, respectively. The lifetime of the green emission band for copolymers **PHF-**

Table 2. Absorption and PL Properties of All the Oligomers and Polymers Both in THF and in Solid Films

	solution λ_{max} (nm)		film λ_{max} (nm)		
compd	abs	PL	abs	PL	Φ_{film}^{PL} (%)
1	350, 306	515	350, 308	542	26
2	367	521	364	535	19
3	373	523	370	534	35
4	378	523, 402 (420)	374	532	46
PHF-FO0.1	380	403 (423)	374	433, 504	18
PHF-FO0.5	380	403 (423)	372	509, 409 (429)	40
PHF-FO1	381	403 (423)	374	513, 411 (432)	56
PHF-FO2	381	402 (423)	374	514, 429	43
PHF-FO5	380	402 (424), 518	373	521	49
PHF-FO10	381	402 (421), 520	372	524	36
PHF-FO25	376	518	368	533	25

Table 3. Fluorescence Decay Lifetimes of All the Oligoflurene and Polyfluorene Derivatives in THF and in Solid Films[a]

	solution			film		
compd	λ_{em} (nm)[b]	τ (ns)[c]	χ^2	λ_{em} (nm)[b]	τ (ns)[c]	χ^2
1	520	8.13	1.085	535	4.93	1.169
2	520	6.95	1.080	535	4.38	1.002
3	520	6.63	1.085	535	4.79	1.036
4	402	0.55	1.074	535	4.92	1.175
	520	6.67	0.977			
PDHF[d]	402	0.46	1.039	550	8.39	1.011
PHF-FO0.1	402	0.43	1.049	505	8.15	1.082
PHF-FO0.5	402	0.49	1.018	510	7.60	1.074
PHF-FO1	402	0.47	1.182	515	7.49	1.051
PHF-FO2	402	0.48	1.070	515	6.51	1.128
	520	6.90	1.178			
PHF-FO5	402	0.50	1.058	520	6.21	1.003
	520	7.02	1.225			
PHF-FO10	402	0.55	1.209	525	5.24	1.220
	520	6.93	1.035			
PHF-FO25	520	6.92	1.157	535	4.21	0.921

[a] Excitation with the maximum absorption. [b] Monitored emission wavelength. [c] Fluorescence lifetime extracted from the single-exponential fits. [d] Thin films after thermal annealing in air at 150 °C for 12 h.

FO2−25 was in the range 6.90−7.02 ns, exhibiting no obvious change with varying fluorenone content. It is noteworthy that the long lifetime of the green emission band for the copolymers was almost identical to that of **2**, which suggested that **2** may be a more appropriate model for the actual chromophore responsible for the green emission in the copolymers.[12g] Figure 7 showed the fluorescence decay curves of the blue and green emission peaks of oligomer **4** in dilute THF solutions for elucidation.

A very similar trend of lifetimes was also observed for the solid-state emission of these materials. The results are also summarized in Table 3. The lifetime of the green emission band for oligomers **(**4−5 ns) were also shorter than that in solutions**.** The increased channels for nonradiative decay tended to generally reduce the lifetime in thin films due to the strong interchain interaction. As for the copolymers, we observed that the lifetime of the green emission band exhibited obvious change with increasing fluorenone content from 8.15 ns for **PHF-FO0.1** to 4.21 ns for **PHF-FO25** (some curves shown in Figure 8). For copolymers **PHF-FO2**, **PHF-FO5**, **PHF-FO10**, and **PHF-FO25**, the green emission also had a shorter lifetime compared with that in solutions; moreover, such difference was enlarged when the fraction of the fluorenone increased from **PHF-FO2** to **PHF-FO25**. The decay of the green emission was a single exponential for all oligomers and copolymers in solid states. In addition, from our measurement, the lifetime of the green emission band from **PDHF** films after high-temperature thermal annealing in air was 8.39 ns and quite close to that for **PHF-FO0.1**. This result suggested that the new green emission from

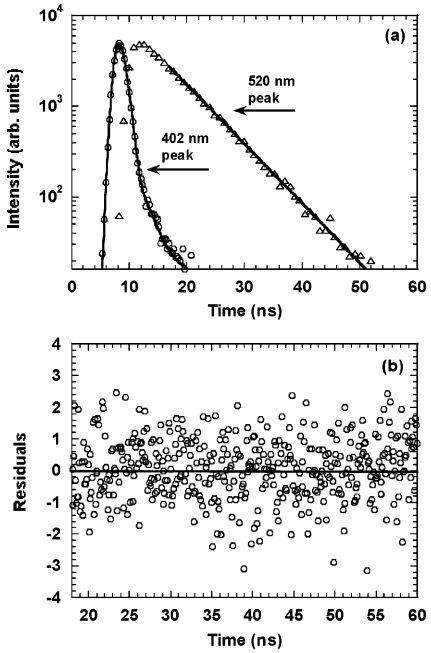

Figure 7. (a) Fluorescence decay curves of the blue and green emission peaks of oligomer **4** in 10^{-5} M THF solution under excitation using absorption λ_{max}. Open symbols represent the actual data, and the solid lines are single-exponential fits to the data. (b) Plot of weighted residuals for the fit corresponding to the 520 nm decay curve.

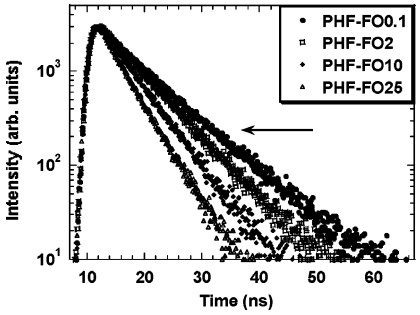

Figure 8. Fluorescence decay curves of the green emission peaks of copolymers **PHF-FO0.1**, **-2**, **-10**, and **-25** in the solid state under excitation using absorption λ_{max}.

air-annealed **PDHF** films might originate from the on-chain ketone defects (less than 0.1 mol %) as a result of the thermal oxidation.

Electroluminescent Properties. To investigate the electroluminescence properties of these oligo- and polyfluorenes, they were used as the emitting layers in double-layer devices with the configuration ITO/PEDOT/materials/Ba/Al, where poly(3,4-ethylene dioxythiophene) (PEDOT) doped with poly(styrenesulfonic acid) (PSS) was used as the hole injection layer. The electroluminescence (EL) spectra are illustrated in Figure 9 and

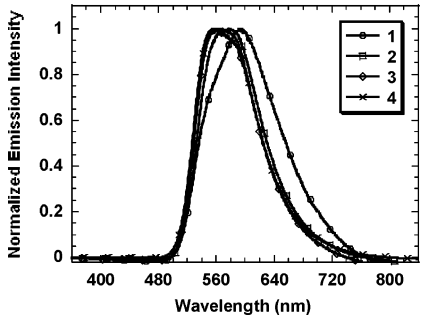

Figure 9. EL spectra of oligomers **1**−**4** from ITO/PEDOT/oligomer/Ba/Al devices.

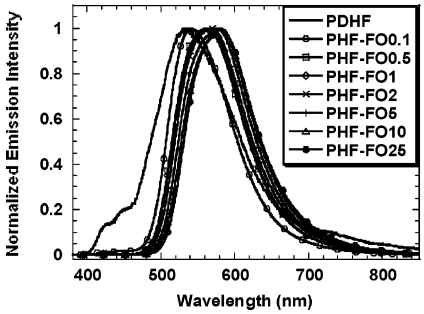

Figure 10. EL spectra of **PDHF** and fluorenone copolymers from ITO/PEDOT/polymer/Ba/Al devices.

Figure 10, respectively. For oligomers **1**−**4**, EL emission consisted exclusively of a yellow emission peak at around 561−594 nm, which was significantly red-shifted in comparison with that of PL spectra. On the other hand, for the EL spectra of the copolymers, a similar yellow emission dominated with an emission peak ranging from 540 nm (for **PHF-FO0.1**) to 579 nm (for **PHF-FO25**), and the blue emission due to the fluorene segments was barely discernible even for the copolymer with fluorenone content as low as 0.1 mol %. The green emission peaks were also progressively red-shifted with increasing fluorenone content in the copolymer; however, the blue emission was completely quenched at much lower concentration of fluorenone moieties, in contrast to the PL spectra in the solid state. The substantial difference between PL and EL spectra implies that different mechanisms are involved in the two processes. This is because the low-energy fluorenone moieties could be excited not only by exciton energy transfer from the fluorene moieties but also by direct charge carrier trapping in the EL device, while they could be excited by energy transfer in PL of thin films.[2d] Such behaviors have also been widely observed during investigating the phosphorescent dye-doped polymer-based guest−host systems as well as PF derivatives incorporated with narrow-band-gap comonomers.[16,18] The EL spectrum of device with **PDHF** was also shown in Figure 10 for comparison. It is noteworthy that the dominant green emission band peak at 533 nm for **PDHF** was quite similar to that of **PHF-FO0.1**. We also found that EL spectra of these fluorenone-containing materials were independent of the driving voltage, indicating a stable emission color with respect to the excitation intensity.

The current−voltage ($I-V$) and luminance−voltage ($L-V$) characteristics as well as the external quantum efficiency as a function of current for the EL devices made with oligomers **1**−**4** are shown in Figure 11. The maximum luminance showed a substantial enhancement from 338 cd/m^2 for **2** to 1430 cd/m^2 for **3**. The device based on **3** and **4** showed a high external quantum efficiency of 0.5−0.6% without significant decay in efficiency over a wide range up to a fairly high current (40 mA). The EL results revealed that the device's performance was greatly enhanced from **1** to **4** with an increase in the efficient conjugation length of the oligomers. The best performance was exhibited by the device using oligomer **3**, which had a maximum luminance of 1430 cd/m^2 and an external quantum efficiency of 0.56% at 12 V with a current density of 376 mA/cm^2.

Figure 12 showed the current−voltage ($I-V$) and luminance−voltage ($L-V$) characteristics as well as the curves of external quantum efficiency as a function of current for the polymer EL

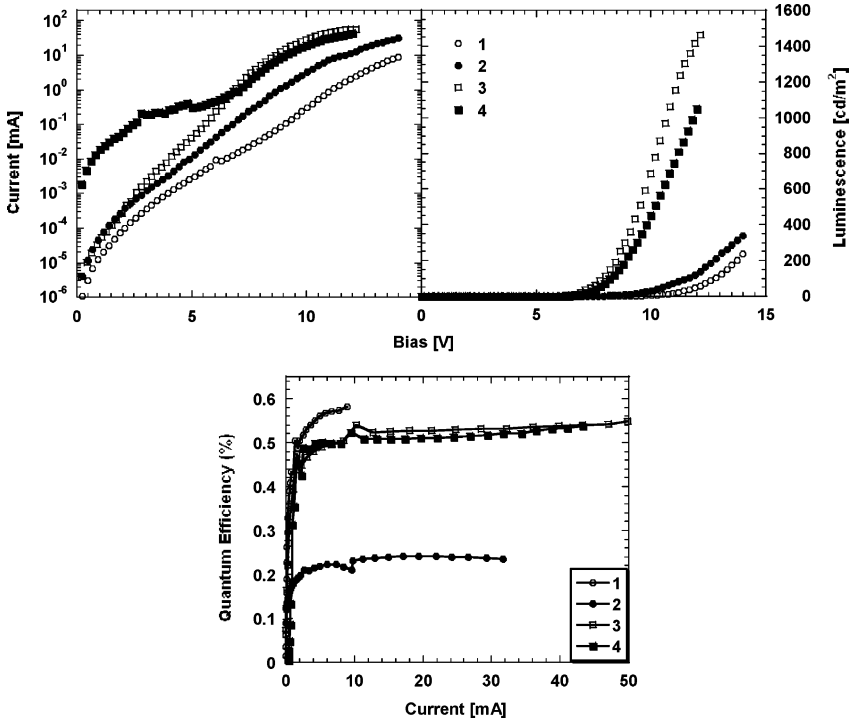

Figure 11. Top: current−voltage ($I-V$) and luminance−voltage ($L-V$) characteristics of ITO/PEDOT/oligomer/Ba/Al devices. Bottom: external quantum efficiency vs current of the top devices.

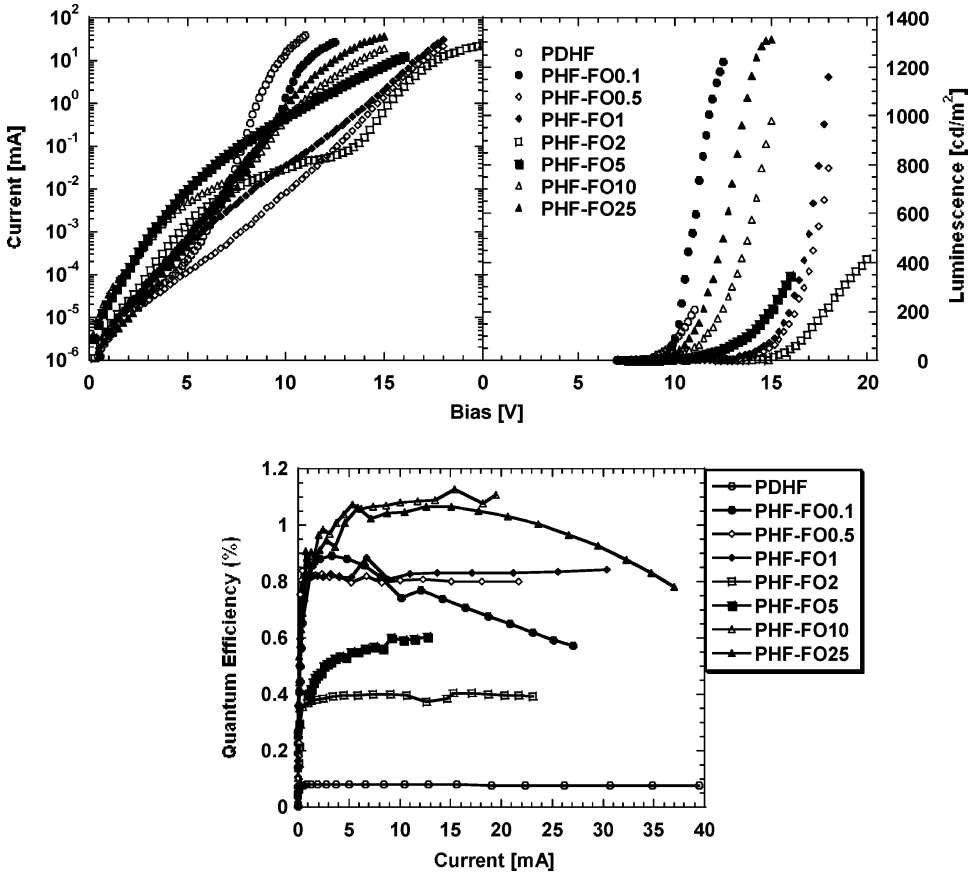

Figure 12. Top: current−voltage (*I*−*V*) and luminance−voltage (*L*−*V*) characteristics of ITO/PEDOT/polymer/Ba/Al devices. Bottom: external quantum efficiency vs current of the top device.

Table 4. Device Performances of All the Fluorenone-Containing Derivatives

	device performances[a]				
compd	EL λ_{max}/nm	*V*/V	*I*/mA	cd/m^{-2}	QE_{max}/%
1	594	14.00	8.96	235.4	0.58
2	580	13.07	21.9	239.6	0.24
3	561	12.00	56.5	1430	0.56
4	562	12.00	43.3	1052	0.54
PDHF	533	9.27	5.07	27.65	0.08
PHF-FO0.1	540	10.35	3.29	232.5	0.89
PHF-FO0.5	561	15.43	2.34	87.66	0.83
PHF-FO1	563	18.00	30.36	1156	0.84
PHF-FO2	565	18.57	15.30	279.7	0.40
PHF-FO5	574	16.00	12.71	346.2	0.60
PHF-FO10	578	14.50	15.36	783.5	1.12
PHF-FO25	579	12.75	12.65	609.1	1.06

[a] Device structure: ITO/PEDOT/oligomer/Ba/Al; active area 0.15 cm^2.

devices. The brightness of the copolymer LEDs was much higher than that of the **PHDF** one. For example, the maximum luminance was 1222, 1156, 978, and 1309 cd/m^2 for **PHF-FO0.1**, **PHF-FO1**, **PHF-FO10**, and **PHF-FO25**, respectively. The maximum external quantum efficiencies of the copolymers were 0.40−1.12% and varied with fluorenone content, which were greatly enhanced comparing with that of **PDHF**. The improved luminance and external quantum efficiency resulted from the better charge recombination efficiency and radiative decay in the fluorenone copolymers, where the fluorenone moieties acted as electron traps and radiative decay sites on the polyfluorene chains. It was noteworthy that the performance of the devices made from **PHF-FO2** and **PHF-FO5** were unsatisfied in comparison with other copolymers although both of them had a higher PL efficiency, which again demonstrated that different operating mechanisms involves in PL and EL processes. The characteristics of all the EL devices are summarized in Table 4.

Conclusion

In conclusion, we have synthesized a series of well-defined 9,9′-dihexylfluorene-*co*-fluorenone copolymers with the fluorenone content ranging from 0.1 to 25 mol % by Suzuki coupling polymerization and used them as model systems to investigate the effect of fluorenone moieties on the photophysics of polyfluorenes for elucidation of the exact origin of the low-energy emission. In addition, we synthesized a set of monodisperse fluorenes oligomers with only one fluorenone unit in the center of the molecules following a repetitive divergent approach and systematically studied their structure−property relationships. The steady-state and time-resolved photoluminescence results of all fluorenone-containing oligomers and copolymers clearly demonstrated that the controversial low-energy emission of the polyfluorenes originated from the intrachain fluorenone defects, definitively ruling out the interchain aggregate or excimer emission based on fluorene segments or fluorenone segments. Furthermore, we found that a fluorenone-centered oligofluorene pentamer (oligomer **2**) was a more appropriate representation of the actual chromophore responsible for the green emission in the copolymers through the study of solution photophysics. The strong intermolecular interaction in the solid state significantly enhanced the intensity of the green emission due to the combined contribution of both the intramolecular and the more efficient intermolecular energy transfer from fluorene segments to fluorenone moieties. Bright yellow EL was achieved from double-layer LEDs based on these materials. The high brightness and external quantum efficiency

of the materials compared with **PDHF** resulted from improved electron injection as well as better carrier transport and the efficient charge trapping and recombination at the fluorenone sites. We have developed a platform to understand the effect of fluorenone on color stability of PFs and further to achieve pure blue emission from conjugated materials based on PFs.

Experimental Section

General Methods. Chemicals were purchased from Aldrich and Acros and used as received. ^{1}H and ^{13}C NMR spectra were recorded on a Mercury plus 300 MHz or Bruker 400 MHz using $CDCl_3$ as solvent in all cases. Elemental analyses were carried out on Elementar Vario EL (Germany). FT-IR spectra were taken on a Nicolet Magna IR-750 spectrometer in a KBr pellet form. GPC was obtained through a Waters GPC 2410 with a refrective index detector in tetrahydrofuran using a calibration curve of polystyrene standards. UV−vis spectra were recorded on a Perkin-Elmer Lambda 35 UV−vis spectrometer. PL spectra were carried out on a Perkin-Elmer LS 55 luminescence spectrometer. Thermogravimetric analysis (TGA) was conducted on SDT 2960 under a heating rate of 10 °C/min from room temperature to 700 °C with an air flow of 100 cm^3/min. Differential scanning calorimetry (DSC) was performed on a Mettler DSC 822^e module in conjunction with a Mettler Thermal Analyst STAR^e system under a heating rate of 10 °C/min and a nitrogen flow rate of 60 cm^3/min. MALDI/TOF (matrix-assisted laser desorption ionization/time-of-flight) MS spectra were recorded with a Bruker BIFLEX III. The PL quantum yields were determined on a Integrating Sphere IS080 with 325 nm excitation from a He−Cd laser (Mells Griod). The time-resolved fluorescence measurements were preformed using the time-correlated single-photon counting technique following excitation by a nanosecond flash lamp (Edinburgh Instruments FL900). EL efficiency and brightness were carried out with calibrated silicon photodiode. PL and EL spectra were recorded on Instaspec 4 CCD spectrophotometer (Oriel Co.).

Device Fabrication and Characterization. LED was fabricated on prepatterned indium−tin oxide (ITO) with sheet resistance 10−20 Ω/sq. The substrate was ultrasonic cleaned with acetone, detergent, deionized water, and 2-propanol. Oxygen plasma treatment was made for 10 min as the final step of substrate cleaning to improve the contact angle just before film coating. Onto the ITO glass was spin-coated a layer of PEDOT:PSS film with thickness of 50 nm from its aqueous dispersion, aiming to improve the hole injection and to avoid the possibility of leakage. PEDOT:PSS film was dried at 80 °C for 2 h in the vacuum oven. The solution of all materials in *p*-xylene was prepared in a nitrogen-filled drybox and spin-coated on top of the ITO/PEDOT:PSS surface. Typical thickness of the emitting layer was 50−80 nm. Then a thin layer of barium as an electron injection cathode and the subsequent 200 nm thick aluminum protection layers were thermally deposited by vacuum evaporation through a mask at a base pressure below 2×10^{-4} Pa. The deposition speed and the thickness of the barium and aluminum layers were monitored by a thickness/rate meter. The cathode area defines the active area of the device. The typical active area of the devices in this study is 0.15 cm^2. The EL layer spin-coating process and the device performance tests were carried out within a glovebox with nitrogen circulation. The luminance of the device was measured with a calibrated photodiode. External quantum efficiency was verified by the measurement of the integrating sphere, and luminance was calibrated after the encapsulation of devices with UV-curing epoxy and thin cover glass.

2,7-Bis(9′,9′-dihexylfluorene-2′-yl)-9-fluorenone (1). To a solution of 2,7-dibromofluorenone (0.91 g, 2.70 mmol) and 2-(9,9-dihexfluorenyl)[1,3,2]dioxaborolane (2.73 g, 6.75 mmol) in toluene (20 mL) was added $Pd(PPh_3)_4$ (1.0 mol %) and 2 M aqueous Na_2CO_3 solution (12 mL). The mixture was degassed and stirred at 90 °C for 20 h and then was poured into a saturated solution of ammonium chloride and extracted with ethyl acetate; the combined organic extracts were washed with brine and dried over $MgSO_4$. After removal of the solvent, the residue was purified by column chromatography using ethyl acetate/petroleum ether as eluent to give 1.59 g (70%) of yellow solids. Further purification could be achieved by recrystallization from chloroform/petroleum ether. ^{1}H NMR ($CDCl_3$, 300 MHz, ppm): 8.03 (2H, d, J = 1.2 Hz, Ar−H), 7.85−7.72 (6H, m, Ar−H), 7.66−7.61 (6H, m, Ar−H), 7.38−7.32 (6H, m, Ar−H), 2.05−2.00 (8H, m, CH_2), 1.15−1.07 (24H, m, CH_2), 0.79−0.74 (12H, t, J = 6.9 Hz, CH_3), 0.68−0.65 (8H, m, CH_2). ^{13}C NMR ($CDCl_3$, 75 MHz, ppm): 194.19, 151.65, 151.02, 142.95, 142.68, 141.15, 140.53, 138.53, 135.25, 133.37, 127.27, 126.83, 125.62, 123.07, 122.92, 121.00, 120.75, 120.07, 119.84, 55.25, 40.44, 31.49, 29.69, 23.77, 22.57, 13.98. Anal. Calcd for $C_{63}H_{72}O$: C, 89.52; H, 8.59. Found: C, 89.12; H, 8.69. MS (MALDI-TOF) *m*/*z*: 844.8 (M^+, 100%).

2,7-Bis(7′-bromo-9′,9′-dihexylfluorene-2′-yl)-9-fluorenone (1a). A mixture of 2,7-bis(9′,9′-dihexylfluorene-2′-yl)-9-fluorenone (1.22 g, 1.44 mmol) and $CuBr_2-Al_2O_3$ (5.98 g, 8.90 mmol) in carbon tetrachloride was stirred at 80 °C for 24 h. The product mixture was filtered off, and the resulting precipitates were washed with carbon tetrachloride. Evaporation of the solvent and purification by recrystallization from chloroform/petroleum ether yielded 1.26 g (87%) of yellow solids. ^{1}H NMR ($CDCl_3$, 300 MHz, ppm): 8.02−8.01 (2H, d, J = 1.5 Hz, Ar−H), 7.83−7.80 (2H, dd, J = 1.5 Hz, J = 7.8 Hz, Ar−H), 7.76−7.73 (2H, d, J = 7.8 Hz, Ar−H), 7.65−7.57 (8H, m, Ar−H), 7.49−7.46 (4H, m, Ar−H), 2.04−1.97 (8H, m, CH_2), 1.16−1.08 (24H, m, CH_2), 0.80−0.75 (12H, t, J = 6.9 Hz, CH_3), 0.66 (8H, m, CH_2). ^{13}C NMR ($CDCl_3$, 75 MHz, ppm): 193.98, 153.22, 151.27, 142.98, 142.42, 140.01, 139.52, 138.97, 135.21, 133.35, 130.05, 126.20, 125.82, 123.02, 121.31, 121.18, 120.97, 120.77, 120.20, 55.59, 40.30, 31.45, 29.58, 23.73, 22.55, 13.97. Anal. Calcd for $C_{63}H_{70}Br_2O$: C, 75.44; H, 7.03. Found: C, 75.39; H, 7.16. MS (MALDI-TOF) *m*/*z*: 1000.5 (M^+, 100%).

2,7-Bis(9′,9′,9″,9″-tetrahexyl-7′,2″-bifluorene-2′-yl)-9-fluorenone (2). The procedure for **1** was followed to prepare **2** from **1a** (1.11 g, 1.11 mmol) as orange solids (1.28 g, 77%). ^{1}H NMR ($CDCl_3$, 300 MHz, ppm): 8.06 (2H, d, J = 1.8 Hz, Ar−H), 7.87−7.74 (12H, m, Ar−H), 7.68−7.63 (12H, m, Ar−H), 7.38−7.33 (6H, m, Ar−H), 2.07−2.02 (16H, m, CH_2), 1.10−1.09 (48H, m, CH_2), 0.79−0.75 (40H, m, CH_2, CH_3). ^{13}C NMR ($CDCl_3$, 75 MHz, ppm): 194.19, 151.96, 151.78, 151.47, 150.99, 142.95, 142.64, 140.81, 140.74, 140.38, 139.69, 138.50, 135.26, 133.37, 127.00, 126.77, 126.20, 126.04, 125.73, 123.06, 122.90, 121.47, 121.40, 121.05, 120.77, 120.15, 120.09, 119.88, 119.72, 55.40, 55.15, 40.36, 31.45, 29.67, 23.82, 23.76, 22.55, 14.00. Anal. Calcd for $C_{113}H_{136}O$: C, 89.86; H, 9.08. Found: C, 89.79; H, 9.10. MS (MALDI-TOF) *m*/*z*: 1508.8 (M^+, 100%).

2,7-Bis(7″-bromo-9′,9′,9″,9″-tetrahexyl-7′,2″-bifluorene-2′-yl)-9-fluorenone (2a). The procedure for **1a** was followed to prepare **2a** from **2** (0.97 g, 0.64 mmol) as orange solids (0.96 g, 90%). ^{1}H NMR ($CDCl_3$, 300 MHz, ppm): 8.06 (2H, d, J = 1.8 Hz, Ar−H), 7.87−7.73 (10H, m, Ar−H), 7.67−7.59 (14H, m, Ar−H), 7.49−7.46 (4H, m, Ar−H), 2.08−1.96 (16H, m, CH_2), 1.15−1.10 (48H, m, CH_2), 0.80−0.75 (40H, m, CH_2, CH_3). ^{13}C NMR ($CDCl_3$, 75 MHz, ppm): 194.16, 153.23, 151.95, 151.83, 151.11, 142.96, 142.62, 140.90, 140.77, 140.57, 139.85, 139.79, 139.26, 138.58, 135.26, 133.37, 129.99, 126.28, 126.20, 125.75, 123.06, 121.46, 121.41, 121.06, 120.99, 120.78, 120.19, 120.13, 120.01, 55.51, 55.41, 40.39, 40.26, 31.45, 31.42, 29.64, 29.59, 23.82, 23.72, 22.54, 13.99. Anal. Calcd for $C_{113}H_{134}Br_2O$: C, 81.36; H, 8.10; Br, 9.58. Found: C, 80.97; H, 7.92. MS (MALDI-TOF) *m*/*z*: 1664.6 (M^+, 100%).

2,7-Bis(9′,9′,9″,9″,9‴,9‴-hexahexyl-7′,2″:7″,2‴-terfluorene-2-yl)-9-fluorenone (3). The procedure for **1** was followed to prepare **3** from **2a** (0.96 g, 0.58 mmol) as pale yellow solids (0.89 g, 71%). ^{1}H NMR ($CDCl_3$, 300 MHz, ppm): 8.07 (2H, s, Ar−H), 7.87−7.64 (36H, m, Ar−H), 7.38−7.32 (6H, m, Ar−H), 2.12−2.04 (24H, m, CH_2), 1.26−1.10 (72H, m, CH_2), 0.86−0.75 (60H, m, CH_2, CH_3). ^{13}C NMR ($CDCl_3$, 75 MHz, ppm): 194.16, 151.96, 151.80, 151.45, 150.97, 142.95, 142.63, 140.84, 140.80, 140.77, 140.56, 140.46, 140.39, 140.33, 140.08, 139.93, 139.73, 138.50, 135.27, 133.35, 126.97, 126.77, 126.16, 126.03, 125.74, 123.05, 122.88, 121.48, 121.40, 121.04, 120.77, 120.13, 119.98, 119.88, 119.70,

55.42, 55.31, 55.14, 40.36, 31.45, 31.43, 29.67, 23.82, 23.76, 22.54, 14.01. Anal. Calcd for $C_{163}H_{200}O$: C, 90.00; H, 9.27. Found: C, 89.77; H, 8.95. MS (MALDI-TOF) *m*/*z*: 2173.0 (M^+, 100%).

2,7-Bis(7‴-bromo-9′,9′,9″,9″,9‴,9‴-hexahexyl-7′,2″:7″,2‴-terfluorene-2-yl)-9-fluorenone (3a). The procedure for **1a** was followed to prepare **3a** from **3** (1.88 g, 0.91 mmol) as pale yellow solids (1.98 g, 94%). ^{1}H NMR ($CDCl_3$, 300 MHz, ppm): 8.06 (2H, s, Ar−H), 7.88−7.59 (36H, m, Ar−H), 7.50−7.46 (4H, m, Ar−H), 2.11−2.01 (24H, m, CH_2), 1.11 (72H, m, CH_2), 0.80−0.76 (60H, m, CH_2, CH_3). ^{13}C NMR ($CDCl_3$, 75 MHz, ppm): 194.13, 153.23, 151.96, 151.81, 151.09, 142.95, 142.62, 140.99, 140.83, 140.77, 140.47, 140.30, 140.11, 139.99, 139.81, 139.75, 139.19, 138.52, 135.27, 133.35, 129.99, 126.19, 125.74, 123.05, 121.48, 121.05, 120.98, 120.77, 120.13, 120.00, 55.50, 55.42, 55.32, 40.33, 31.46, 31.42, 29.66, 29.62, 23.83, 23.73, 22.54, 14.00. Anal. Calcd for $C_{163}H_{198}Br_2O$: C, 83.91; H, 8.55. Found: C, 83.61; H, 8.64. MS (MALDI-TOF) *m*/*z*: 2328.6 (M^+, 100%).

2,7-Bis(9′,9′,9″,9″,9‴,9‴,9⁗,9⁗-octahexyl-7′,2″:7″,2‴:7‴,2⁗-tetrafluorene-2-yl)-9-fluorenone (4). The procedure for **1** was followed to prepare **4** from **3a** (0.38 g, 0.16 mmol) as pale yellow solids (0.36 g, 78%). ^{1}H NMR ($CDCl_3$, 300 MHz, ppm): 8.07 (2H, s, Ar−H), 7.85−7.66 (48H, m, Ar−H), 7.38−7.34 (6H, m, Ar−H), 2.11 (32H, m, CH_2), 1.13 (96H, m, CH_2), 0.78 (80H, m, CH_2, CH_3). ^{13}C NMR ($CDCl_3$, 75 MHz, ppm): 194.10, 151.98, 151.80, 151.46, 150.99, 142.95, 142.65, 140.84, 140.50, 140.34, 139.99, 139.76, 138.53, 135.30, 133.35, 127.99, 126.97, 126.80, 126.18, 125.77, 123.03, 122.90, 121.50, 121.05, 120.77, 119.99, 119.72, 55.44, 55.33, 55.15, 40.37, 31.45, 29.67, 23.84, 22.55, 14.03, 13.99. Anal. Calcd for $C_{213}H_{264}O$: C, 90.07; H, 9.37. Found: C, 89.81; H, 9.37. MS (MALDI-TOF) *m*/*z*: 2831.6 ($M^+ + 3$, 100%).

General Procedure of Polymerization. Under a nitrogen atmosphere, 9,9-dihexylfluorene-2,7-bis(trimethylene boronate), 2,7-dibromo-9,9-dihexylfluorene, and/or 2,7-bis(7′-bromo-9′,9′-dihexylfluorene-2′-yl)-9-fluorenone (**1a**) were mixed together with 1.5 mol % of $Pd(PPh_3)_4$, degassed toluene, and 2 M aqueous sodium carbonate solution. The mixture was vigorously stirred at 80−90 °C for 48 h. The mixture was poured into stirred 100 mL of methanol to precipitate a plenty of solids. The solid was collected by filtration and washed with methanol and water. The polymer was further purified by washing with refluxing acetone in Soxhlet for 2 days and was dried under vacuum at room temperature to afford the desired polymers. The resulting materials were soluble in THF, chloroform, and toluene. Yield: ∼70−80%.

PHF-FO0.1. ^{1}H NMR ($CDCl_3$, 300 MHz, ppm): 7.87−7.84 (2H, m, Ar−H), 7.72−7.68 (4H, m, Ar−H), 2.12 (4H, br, CH_2), 1.14 (12H, br, CH_2), 0.81−0.77 (10H, m, CH_2 and CH_3). ^{13}C NMR ($CDCl_3$, 75 MHz, ppm): 151.80, 140.52, 140.01, 128.78, 127.20, 126.16, 121.51, 119.98, 55.33, 40.36, 31.46, 29.67, 23.84, 22.55, 14.02. Anal. Calcd for $C_{24.988}H_{31.974}O_{0.001}$: C, 90.30; H, 9.70. Found: C, 89.88; H, 9.32.

PHF-FO0.5. ^{1}H NMR ($CDCl_3$, 300 MHz, ppm): 7.87−7.80 (2H, m, Ar−H), 7.72−7.61 (4H, m, Ar−H), 2.12 (4H, br, CH_2), 1.14 (12H, br, CH_2), 0.80−0.78 (10H, m, CH_2 and CH_3). ^{13}C NMR ($CDCl_3$, 75 MHz, ppm): 151.80, 140.52, 140.01, 128.77, 127.19, 126.16, 121.52, 119.99, 55.32, 40.35, 31.45, 29.65, 23.82, 22.55, 14.01. Anal. Calcd for $C_{24.94}H_{31.843}O_{0.005}$: C, 90.30; H, 9.68. Found: C, 89.91; H, 9.77.

PHF-FO1. ^{1}H NMR ($CDCl_3$, 300 MHz, ppm): 7.87−7.80 (2H, m, Ar−H), 7.70−7.62 (4H, m, Ar−H), 2.12 (4H, br, CH_2), 1.14 (12H, br, CH_2), 0.80−0.77 (10H, m, CH_2 and CH_3). ^{13}C NMR ($CDCl_3$, 75 MHz, ppm): 151.82, 140.56, 140.34, 140.03, 132.21, 132.09, 128.77, 128.53, 128.38, 127.19, 126.17, 121.54, 119.98, 55.60, 55.34, 40.37, 31.45, 29.66, 23.86, 22.54, 14.00. Anal. Calcd for $C_{24.88}H_{31.74}O_{0.01}$: C, 90.29; H, 9.67. Found: C, 89.78; H, 9.13.

PHF-FO2. ^{1}H NMR ($CDCl_3$, 300 MHz, ppm): 8.08 (0.04H, s, Ar−H), 7.87−7.80 (2.04H, m, Ar−H), 7.69−7.62 (4.04H, m, Ar−H), 2.35 (4H, br, CH_2), 1.14 (12H, br, CH_2), 0.80 (10H, br, CH_2 and CH_3). ^{13}C NMR ($CDCl_3$, 75 MHz, ppm): 194.23, 152.29, 151.81, 151.70, 141.92, 141.74, 140.53, 140.32, 140.02, 132.21, 132.08, 131.87, 131.30, 128.77, 128.53, 128.36, 127.19, 126.16, 121.52, 120.77, 119.99, 55.60, 55.33, 40.36, 31.45, 29.66, 23.84, 22.56, 14.02. Anal. Calcd for $C_{24.76}H_{31.48}O_{0.02}$: C, 90.27; H, 9.63. Found: C, 90.01; H, 9.25.

PHF-FO5. ^{1}H NMR ($CDCl_3$, 300 MHz, ppm): 8.08 (0.1H, s, Ar−H), 7.87−7.80 (2.1H, m, Ar−H), 7.72−7.64 (4.1H, m, Ar−H), 2.17−2.12 (4H, br, CH_2), 1.14 (12H, br, CH_2), 0.87−0.77 (10H, m, CH_2 and CH_3). ^{13}C NMR ($CDCl_3$, 75 MHz, ppm): 194.25, 152.28, 151.80, 151.34, 144.64, 142.96, 142.67, 141.91, 141.71, 140.80, 140.50, 140.00, 138.99, 138.53, 135.28, 133.38, 132.20, 132.06, 131.26, 128.78, 128.54, 128.38, 127.19, 126.70, 126.15, 125.77, 123.10, 121.50, 121.08, 120.78, 119.98, 55.60, 55.42, 55.32, 40.36, 31.45, 29.66, 23.83, 22.55, 14.02. Anal. Calcd for $C_{24.4}H_{30.7}O_{0.05}$: C, 90.23%; H, 9.53%. Found: C, 90.55; H, 9.32.

PHF-FO10. ^{1}H NMR ($CDCl_3$, 300 MHz, ppm): 8.08−8.06 (0.22H, m, Ar−H), 7.86−7.80 (2.22H, m, Ar−H), 7.72−7.62 (4.22H, m, Ar−H), 2.17−2.12 (4H, br, CH_2), 1.14 (12H, br, CH_2), 0.80−0.78 (10H, m, CH_2 and CH_3). ^{13}C NMR ($CDCl_3$, 75 MHz, ppm): 194.20, 152.28, 151.97, 151.80, 151.45, 144.63, 142.97, 142.66, 141.89, 141.70, 140.84, 140.51, 140.01, 139.73, 138.52, 135.28, 133.40, 132.20, 132.06, 131.90, 131.33, 128.77, 128.55, 128.38, 127.18, 126.15, 125.75, 123.07, 121.50, 121.06, 120.79, 119.98, 55.42, 55.32, 55.14, 40.36, 31.45, 29.66, 23.82, 22.55, 14.02. Anal. Calcd for $C_{23.8}H_{29.4}O_{0.1}$: C, 90.15; H, 9.35. Found: C, 89.86; H, 9.39.

PHF-FO25. ^{1}H NMR ($CDCl_3$, 300 MHz, ppm): 8.08−8.06 (0.66H, m, Ar−H), 7.87−7.79 (2.66H, m, Ar−H), 7.70 (4.66H, m, Ar−H), 2.12 (4H, br, CH_2), 1.13 (12H, br, CH_2), 0.79 (10H, br, CH_2 and CH_3). ^{13}C NMR ($CDCl_3$, 75 MHz, ppm): 194.18, 152.43, 151.95, 151.80, 151.34, 144.38, 143.24, 142.94, 142.64, 142.26, 141.67, 140.83, 140.42, 140.03, 139.73, 138.52, 135.26, 133.38, 132.17, 132.04, 131.89, 131.15, 128.76, 128.53, 128.38, 127.17, 126.79, 126.20, 125.95, 125.73, 123.09, 121.49, 121.05, 120.83, 120.16, 55.69, 55.41, 55.32, 40.42, 31.46, 29.66, 23.83, 22.56, 14.01. Anal. Calcd for $C_{22}H_{22.5}O_{0.25}$: C, 89.90; H, 8.74. Found: C, 89.52; H, 8.79.

Acknowledgment. This research was financially supported by the Major State Basic Research Development Program (No. 2002CB613402) from the Minister of Science and Technology, and National Natural Science Foundation of China (NSFC. 20425207, 50473016, and 90201021).

References and Notes

(1) (a) Scherf, U.; List, E. J. W. *Adv. Mater.* **2002**, *14*, 477. (b) Neher, D. *Macromol. Rapid Commun.* **2001**, *22*, 1365. (c) Sainova, D.; Miteva, T.; Nothofer, H. G.; Scherf, U.; Glowacki, I.; Ulanski, J.; Fujikawa, H.; Neher, D. *Appl. Phys. Lett.* **2000**, *76*, 1810. (d) Gross, M.; Müller, D. C.; Nothofer, H.-G.; Scherf, U.; Neher, D.; Bräuchle, C.; Meerholz, K. *Nature (London)* **2000**, *405*, 661.

(2) (a) Bliznyuk, V. N.; Carter, S. A.; Scott, J. C.; Klärner, G.; Miller, R. D.; Miller, D. C. *Macromolecules* **1999**, *32*, 361. (b) Weinfurtner, K.-H.; Fujikawa, H.; Tokito, S.; Taga, Y. *Appl. Phys. Lett.* **2000**, *76*, 2502. (c) Zeng, G.; Yu, W.-L.; Chua, S.-J.; Huang, W. *Macromolecules* **2002**, *35*, 6907. (d) List, E. J. W.; Güntner, R.; Scanducci de Freitas, P.; Scherf, U. *Adv. Mater.* **2002**, *14*, 374. (e) Gong, X.; Iyer, P. K.; Moses, D.; Bazan, G. C.; Heeger, A. J.; Xiao, S. S. *Adv. Funct. Mater.* **2003**, *13*, 325.

(3) Lemmer, U.; Heun, S.; Mahrt, R. F.; Scherf, U.; Hopmeier, M.; Sieger, U.; Göbel, E. O.; Müllen, K.; Bässler, H. *Chem. Phys. Lett.* **1995**, *240*, 373.

(4) (a) Setayesh, S.; Grimsdale, A. C.; Weil, T.; Enkelmann, V.; Müllen, K.; Meghdadi, F.; List, E. J. W.; Leising, G. *J. Am. Chem. Soc.* **2001**, *123*, 946. (b) Marsitzky, D.; Vestberg, R.; Blainey, P.; Tang, B. T.; Hawker, C. J.; Carter, K. R. *J. Am. Chem. Soc.* **2001**, *123*, 6965. (c) Ego, C.; Grimsdale, A. C.; Uckert, F.; Yu, G.; Srdanov, G.; Müllen, K. *Adv. Mater.* **2002**, *14*, 809. (d) Chou, C. H.; Shu, C. F. *Macromolecules* **2002**, *35*, 9673. (e) Wu, F.-I.; Reddy, D. S.; Shu, C.-F.; Liu, M. S.; Jen, A. K.-Y. *Chem. Mater.* **2003**, *15*, 269. (f) Shu, C.-F.; Dodda, R.; Wu, F.-I.; Liu, M. S.; Jen, A. K.-Y. *Macromolecules* **2003**, *36*, 6698.

(5) (a) Klärner, G.; Davey, M. H.; Chen, W.-D.; Scott, J. C.; Miller, R. D. *Adv. Mater.* **1998**, *10*, 993. (b) Yu, W.-L.; Cao, Y.; Pei, J.; Huang, W.; Heeger, A. J. *Appl. Phys. Lett.* **1999**, *75*, 3270. (c) Yu, W.-L.; Pei, J.; Huang, W.; Heeger, A. J. *Adv. Mater.* **2000**, *12*, 828. (d) Jiang, X. Z.; Liu, S.; Ma, H.; Jen, A. K.-Y. *Appl. Phys. Lett.* **2000**, *76*, 1813.

(e) Lu, J. P.; Tao, Y.; D'iorio, M.; Li, Y. N.; Ding, J. F.; Day, M. *Macromolecules* **2004**, *37*, 2442.
(6) (a) Klärner, G.; Miller, R. D.; Hawker, C. J. *Polym. Prepr.* **1998**, 1047. (b) Miteva, T.; Meisel, A.; Knoll, W.; Nothofer, H. G.; Scherf, U.; Müller, D. C.; Meerholz, K.; Yasuda, A.; Neher, D. *Adv. Mater.* **2001**, *13*, 565. (c) Lee, J. L.; Hwang, D. H.; Park, H.; Do, L. M.; Chu, H. Y.; Zyung, T.; Miller, R. D. *Synth. Met.* **2000**, *111*, 195.
(7) (a) Klaener, G.; Lee, J. L.; Lee, V. Y.; Chan, E.; Chen, J. P.; Nelson, A.; Markiewicz, D.; Siemens, R.; Scott, J. C.; Miller, R. D. *Chem. Mater.* **1999**, *11*, 1800. (b) Chen, J. P.; Klaerner, G.; Lee, J. I.; Markiewicz, D.; Lee, V. Y.; Miller, R. D.; Scott, J. C. *Synth. Met.* **1999**, *107*, 129. (c) Cho, H. J.; Jung, B. J.; Cho, N. S.; Lee, J.; Shim, H. K. *Macromolecules* **2003**, *36*, 6704.
(8) (a) Gaal, M.; List, E. J. W.; Scherf, U. *Macromolecules* **2003**, *36*, 4236. (b) Romaner, L.; Pogantsch, A.; de Freitas, P. S.; Scherf, U.; Gaal, M.; Zoher, E.; List, E. J. W. *Adv. Funct. Mater.* **2003**, *13*, 597.
(9) Zhao, W.; Cao, T.; White, J. M. *Adv. Funct. Mater.* **2004**, *14*, 783.
(10) Lupton, J. M.; Craig, M. R.; Meijer, E. W. *Appl. Phys. Lett.* **2002**, *80*, 4489.
(11) (a) Lupton, J. M.; Klein, J. *Phys. Rev. B* **2002**, *65*, 193202. (b) Li, J.; Li, M.; Bo, Z.-S. *Chem.—Eur. J.* **2005**, *11*, 6930. (c) Chi, C.-Y.; Im, C.; Enkelmann, V.; Ziegler, A.; Lieser, G.; Wegner, G. *Chem.—Eur. J.* **2005**, *11*, 6833.
(12) (a) Lee, J.-K.; Klaerner, G.; Miller, R. D. *Chem. Mater.* **1999**, *11*, 1083. (b) Panozzo, S.; Vial, J.-C.; Kervella, Y.; Stéphan, O. *J. Appl. Phys.* **2002**, *92*, 3495. (c) Zojer, E.; Pogantsch, A.; Hennebicq, E.; Beljonne, D.; Brédas, J. L.; Scandiucci de Freitas, P.; Scherf, U.; List, E. J. W. *J. Chem. Phys.* **2002**, *117*, 6794. (d) Hintschich, S. I.; Rothe, C.; Sinha, S.; Monkman, A. P.; Scandiucci de Freitas, P.; Scherf, U. *J. Chem. Phys.* **2003**, *118*, 12017. (e) Gong, X.; Moses, D.; Heeger, A. J.; Xiao, S. *Synth. Met.* **2004**, *141*, 17. (f) Kulkarni, A. P.; Kong, X.; Jenekhe, S. A. *J. Phys. Chem. B* **2004**, *108*, 8689.
(13) Sims, M.; Bradley, D. D. C.; Ariu, M.; Koeberg, M.; Asimakis, A.; Grell, M.; Lidzey, D. G. *Adv. Funct. Mater.* **2004**, *14*, 765.
(14) Zhou, X.-H.; Yan, J.-C.; Pei, J. *Org. Lett.* **2003**, *5*, 3543.
(15) Klaerner, G.; Miller, R. D. *Macromolecules* **1998**, *31*, 2007.
(16) (a) Yang, R. Q.; Tian, R. Y.; Hou, Q.; Yang, W.; Cao, Y. *Macromolecules* **2003**, *36*, 7453. (b) Yang, J.; Jiang, C. Y.; Zhang, Y.; Yang, R. Q.; Yang, W.; Hou, Q.; Cao, Y. *Macromolecules* **2004**, *37*, 1211.
(17) Teetsov, J.; Fox, M. A. *J. Mater. Chem.* **1999**, *9*, 2117.
(18) (a) Gong, X.; Robinson, M. R.; Ostrowski, J. C.; Moses, D.; Bazan, G. C.; Heeger, A. J. *Adv. Mater.* **2002**, *14*, 581. (b) Gong, X.; Ostrowski, J. C.; Moses, D.; Bazan, G. C.; Heeger, A. J. *Adv. Mater.* **2002**, *14*, 581.

MA0601262